Supplementary Material for

Rudimentary G-quadruplex-based telomere capping in *Saccharomyces cerevisiae.*

Jasmine S. Smith[1,2], Qijun Chen[1], Liliya A. Yatsunyk[3], John M. Nicoludis[3], Mark S. Garcia[1,2-], Ramon Kranaster[4], Shankar Balasubramanian[4,5,6], David Monchaud[7], Marie-Paule Teulade-Fichou[7], Lara Abramowitz[1,2], David C. Schultz[8], and F. Brad Johnson[1,2,9]

[1]Department of Pathology and Laboratory Medicine, [2]Cell and Molecular Biology Group, Biomedical Graduate Studies. University of Pennsylvania School of Medicine, Philadelphia, PA 19104, USA.

[3]Department of Chemistry and Biochemistry, Swarthmore College. Swarthmore, PA 19081, USA.

[4]Department of Chemistry, University of Cambridge, Cambridge CB2 1EW, UK.

[5] School of Clinical Medicine, University of Cambridge, Cambridge CB2 OSP, UK

[6] Cancer Research UK Cambridge Research Institute, Li Ka Shing Centre, Cambridge CB2 ORE, UK

[7]Institut Curie, Section Recherche, CNRS, UMR176, Centre Universitaire Paris XI, Bat. 110, 91405 Orsay, France.

[8]Protein Expression, Libraries, and Molecular Screening Facility. The Wistar Institute. Philadelphia PA 19104, USA.

[9]Corresponding author.
405A Stellar-Chance Labs
422 Curie Boulevard
University of Pennsylvania
Philadelphia, PA 19104-6100
Tel: 215-573-5037
Fax: 215-573-6317
Email: johnsonb@mail.med.upenn.edu

Supplementary Figure 1a-f

a

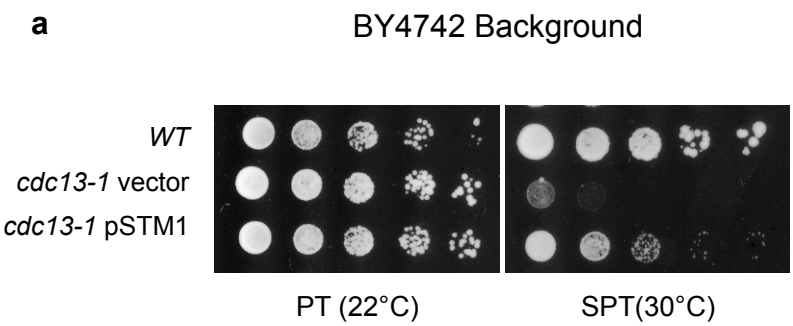

b

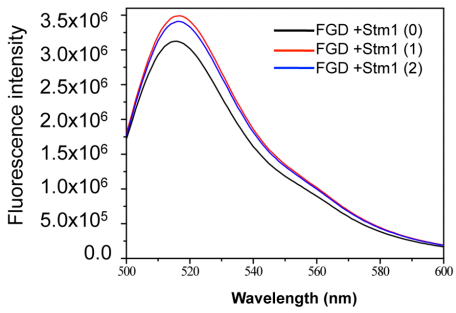

c

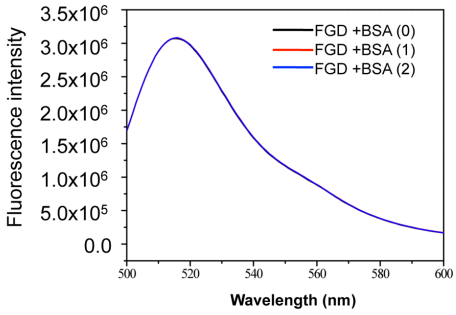

d

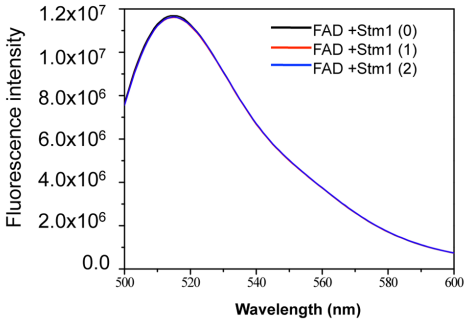

e

Oligo Name	Sequence
1-corr	GGG TGT GGT GTG TGT GGG TGT GGT GGG TGT GG
2-corr	GGG TGT GGT GGG TGT GTG GGT GTG GGT G
3-corr	GGG TGT GGG TGT GTG GGT GTG GGT GTG G
4-corr	GGG TGT GGT GTG TGG GTG TGG GTG TGG G

f

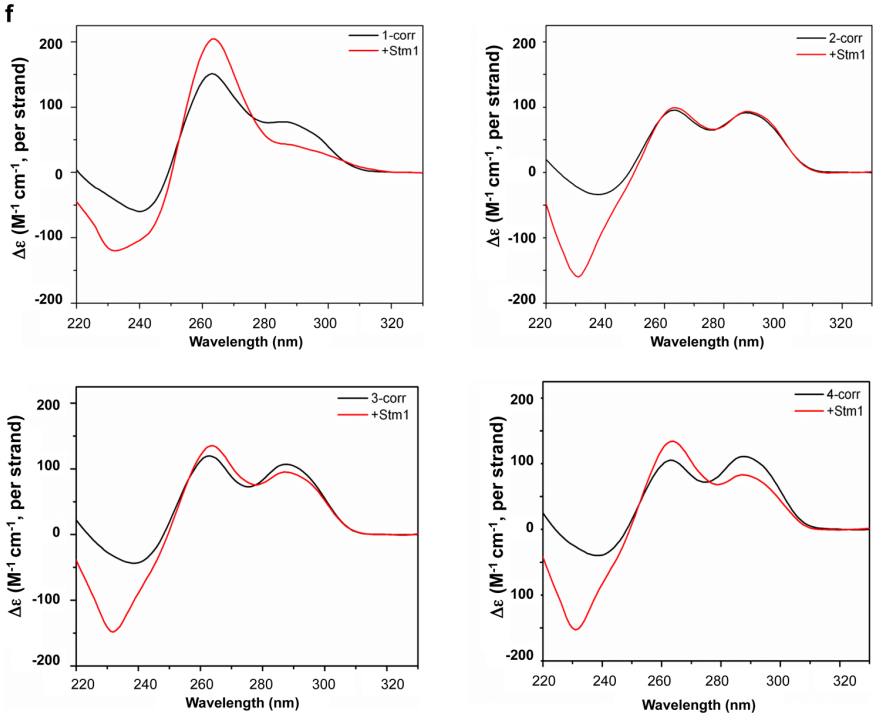

Supplementary Figure 1g-k

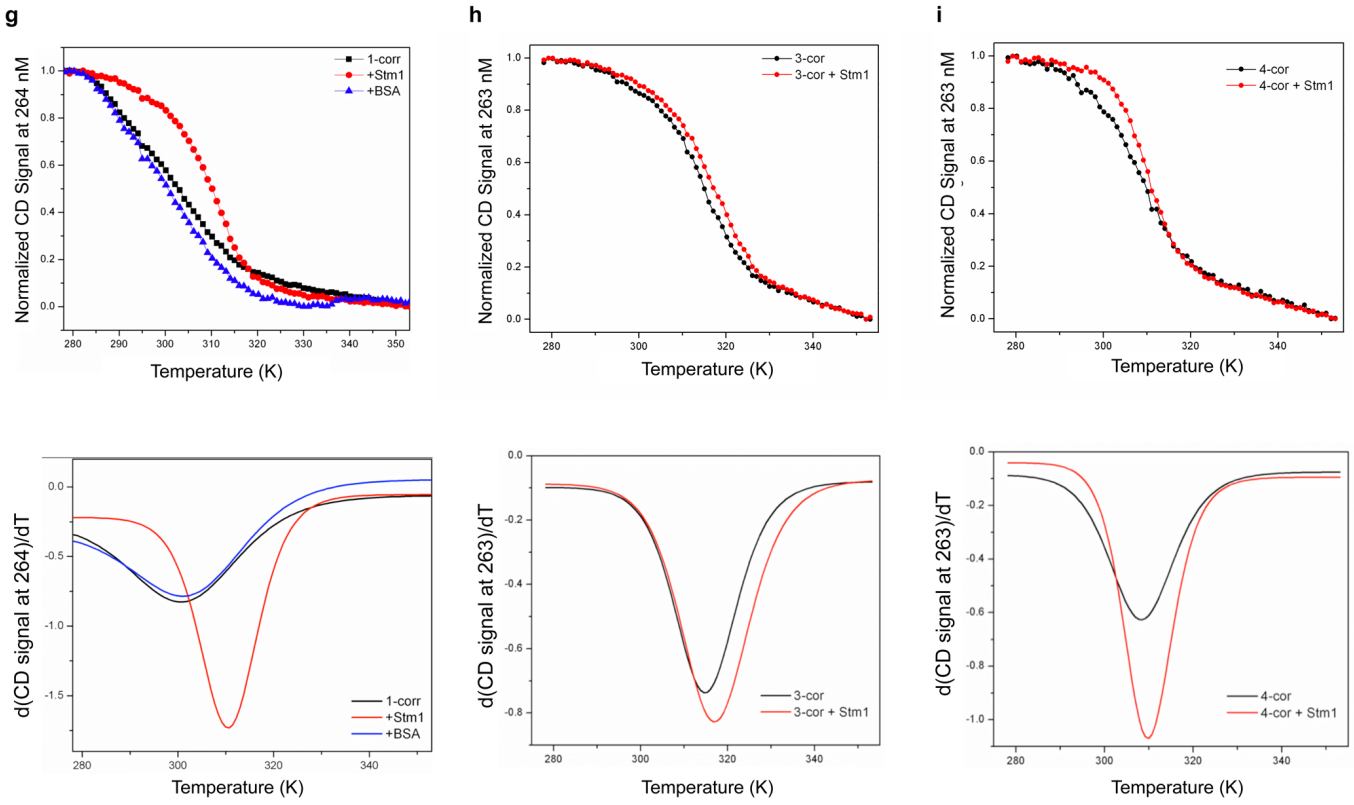

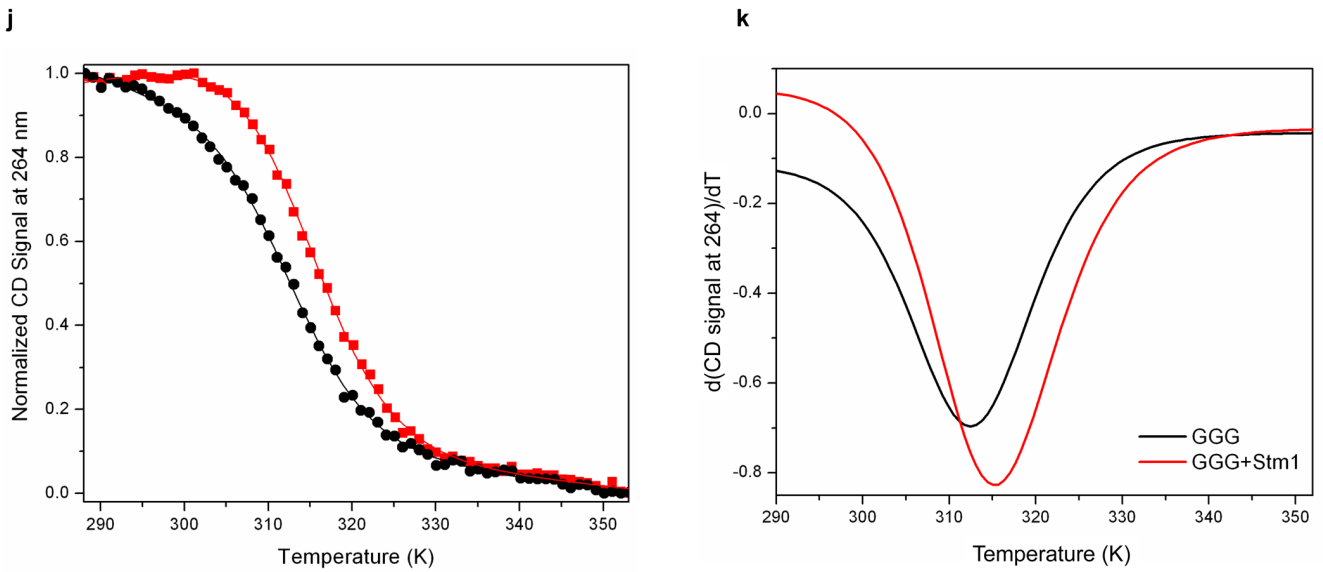

Supplementary Figure 1. Stm1-based rescue of *cdc13-1* is not strain-specific and correlates with stabilization of G4 DNA. (a) Rescue of the *cdc13-1* ts growth defect by pSTM1 is not specific to the PSY316 background as it can be recapitulated in the BY4742 background. Growth of *cdc13-1* strains expressing pSTM1 or vector control spotted at 10^5 cells and ten-fold serial dilutions and grown on SC-LEU at the indicated temperatures for 3 days. **(b-c)** FRET analysis to assess the interaction between a model yeast telomere sequence, FGD (Fam-GGG $(TGTGGG)_3$-Dab), and Stm1 (b) or BSA (c). Changes in fluorescence with added protein indicate interaction between DNA and the protein. **(d)** FRET analysis of the non-G4 control sequence FAD (Fam-GAG$(TGTGAG)_3$-Dab) with or without Stm1. For each FRET experiment, annealed and labeled oligo was diluted to 0.2 μM in TEM buffer with 100 mM KCl at 25°C with no added protein (*0*), or 8 equivalents of protein and analyzed immediately (*1*) or after a one hour incubation (*2*). We note that the increased fluorescence induced by Stm1 is likely due to binding of Stm1 to the G4 DNA, which in turn somehow disrupts interaction between the fluorophore and quencher (see below).
(e) Telomere sequences tested for G4 DNA formation using circular dichroism (based on sequencing of telomeric DNA from clones in **Table 1**). **(f)** Circular dichroism spectra of indicated oligos in buffer alone (10 mM Li cacodylate, 99 mM LiCl, 1 mM KCl, pH 7.2) or buffer with two equivalents of Stm1 protein. **(g,h,i)** Stabilization of 1-corr, 3-corr, and 4-corr telomeric sequences by Stm1 (by +9.8, 2.3, and 1.8°C respectively), as determined by melting of the G4 DNA. The curves at the *top* show the change in peak CD signal vs. increasing temperature at the indicated wavelengths, and the curves at the *bottom* show the first derivatives of the melting curves; the peak minima were used to calculate the difference in melting temperatures of the G4 DNA without *vs*. with Stm1. As a control, 1-corr was tested in the presence of BSA, and showed a non-significant G4 DNA stabilization of +0.1°C. **(j)** CD melting curves of 2.52 μM GGG $(TGTGGG)_3$ (i.e. the "GGG" oligo) alone (*black*) or with two equivalents of Stm1 (*red*) under low potassium (1 mM KCl) conditions monitored at 264 nm. **(k)** First derivative of melting curves, fit using the Marky-Breslauer two state model. The minimum signifies melting temperature. Stm1 stabilized the GGG oligo by +2.9°C, whereas BSA-induced stabilization was not significant (+0.3°C, *not shown*).

Supplementary Figure 2

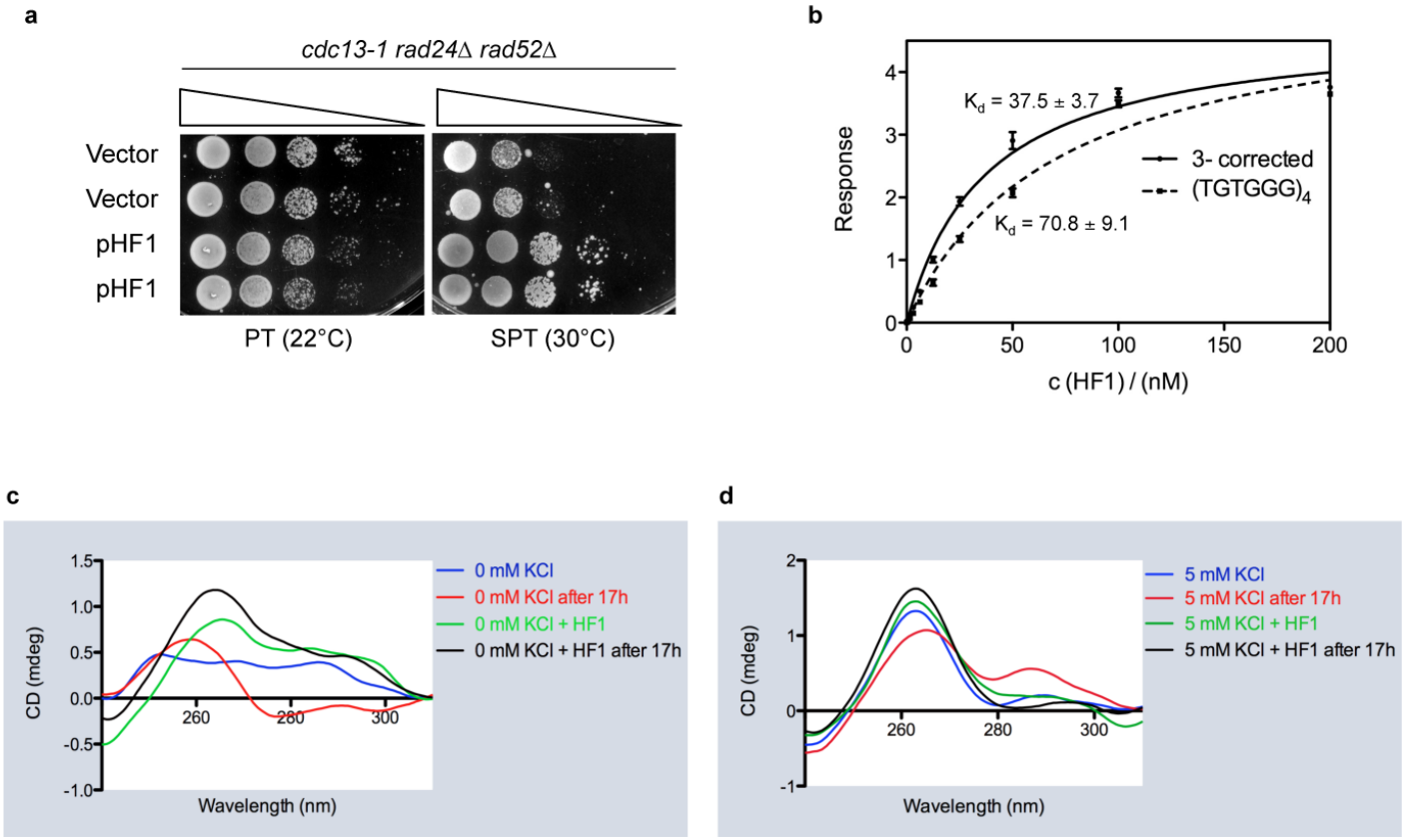

Supplementary Figure 2. The G4 DNA scFv antibody, HF1, rescues the *cdc13-1* ts phenotype in a *rad52*Δ *rad24*Δ background and stabilizes telomere G4 DNA. (a) 10^5 cells and ten-fold serial dilutions of the *cdc13-1 rad24*Δ *rad52*Δ strains overexpressing HF1 or with vector control were grown on SC-HIS containing 2% galactose at PT or NPT for 3 days. **(b)** ELISA assay, were performed as described[13], to determine equilibrium dissociation constants (K_d) of HF1 from two different model yeast telomere G-quadruplexes: 5´-biotin-$(TGTGGG)_4$-3´ and '3-corrected' 5´-biotin-GGGTGTGGGTGTGTGGGTGTGGGTGTGG-3´ (see **Table 1**). HF1 shows a high affinity for both yeast telomeric sequences with K_d values in the 35-75 nM range, and comparable to the c-kit2 genomic G-quadruplex (K_d 54 nM), which was employed in the original phage selection experiments that generated HF1 **(c-d)** Circular dichroism spectra of a model yeast telomere sequence $(TGTGGG)_4$ (i.e. the "GGG" oligo) at 0 mM or low (5 mM) KCl in the in absence or presence of one equivalent of the G-quadruplex binding antibody HF1. Characteristic G4 DNA signal increases in the presence of HF1, particularly in the absence of KCl.

Supplementary Figure 3

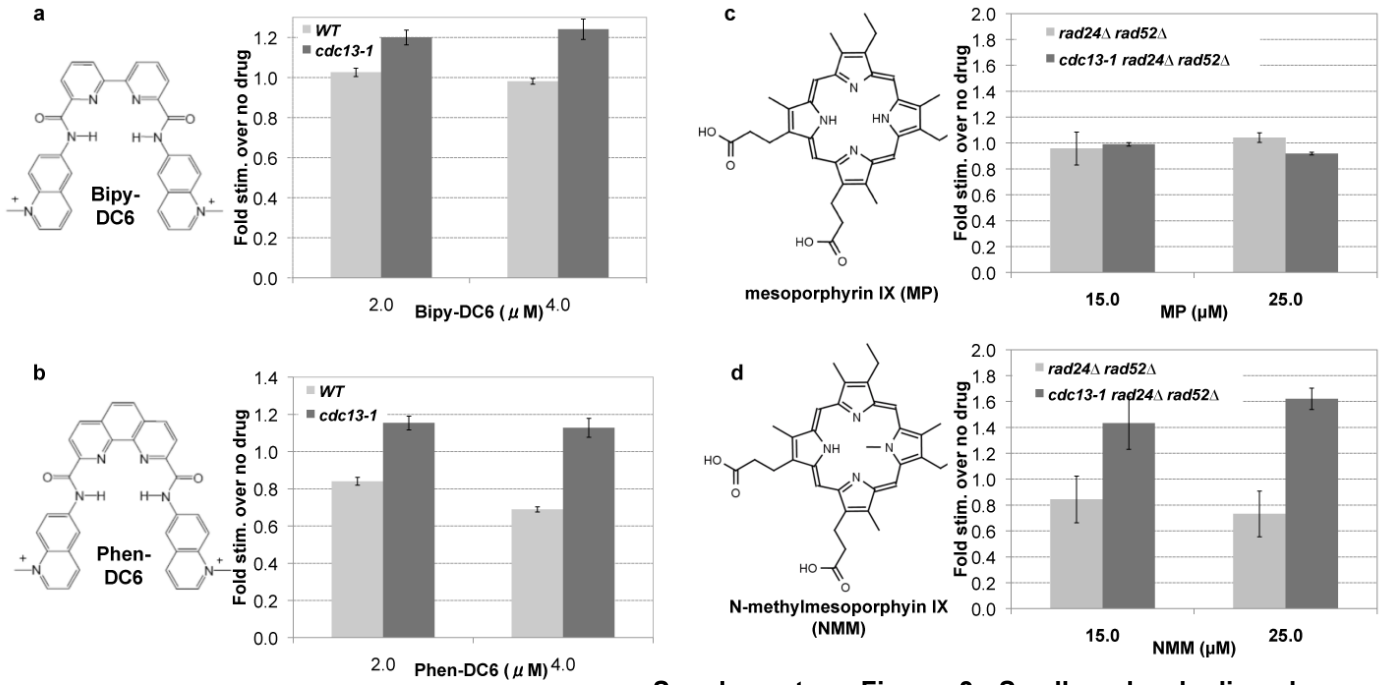

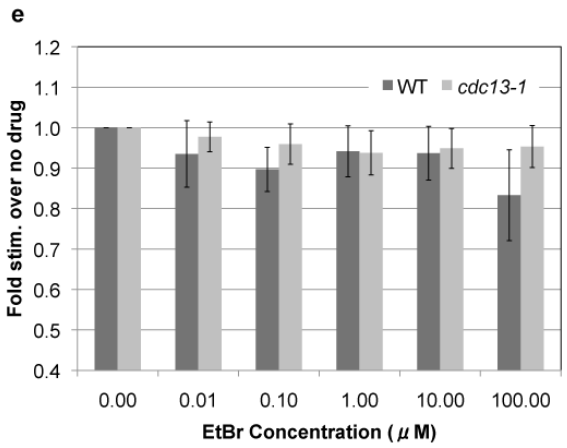

Supplementary Figure 3. Small molecule ligands that selectively stabilize G4 DNA stimulate growth of *cdc13-1* cells at SPT.

(a, b) Treatment of *cdc13-1* or WT cells with two related G-quadruplex stabilizing compounds Bipy-DC6 and Phen-DC6. Growth stimulation by drug was normalized to DMSO vehicle controls. Drug concentrations $\geq$ 8 μM inhibited growth in both genotypes. Differences between *cdc13-1* and *WT* for Bipy-DC6 trended toward significance at 2 μM, p = 0.10, and were significant at 4 μM, p = 0.03, whereas differences were significant for the stronger G-quadruplex stabilizing ligand Phen-DC6 at both 2 μM (p = 0.02) and 4 μM (p = 0.01) **(c, d)** Treatment of *cdc13-1 rad24Δ rad52Δ* cells with a non-G4 DNA specific porphyrin, mesoporphyrin IX (MP) **(c),** or a highly selective G4 DNA ligand, *N*-methylmesoporphyrin IX (NMM). **(d)** Growth in the presence of MP and NMM was normalized to H_2O vehicle controls. Differences between *cdc13-1* and *WT* growth were not significant for MP: p = 0.54 at 15 μM and p = 0.06 at 25 μM; but differences between *cdc13-1* and *WT* growth were significant for NMM at 25 μM, p = 0.04, and trended toward significance at 15 μM, p = 0.16. **(e)** Wild type or cdc13-1 cells were grown with the indicated concentrations of the duplex-DNA binding agent ethidium bromide (EtBr). Note that the growth of wild type and *cdc13-1* mutant cells was inhibited similarly. For all experiments, log growth cultures were diluted to 4 x 10^5 cells/ml and then grown for 24 (NMM, MP) or 30 hours (Bipy-DC6, Phen-DC6, EtBr). Experiments were performed in duplicate (Phen-DC6, MP, NMM, EtBr) or triplicate (Bipy-DC6) with the indicated concentrations of drug, p values were calculated using unpaired two sample Student's t-tests, and standard errors are shown.

In addition, we estimated the intracellular concentration of NMM in cells grown in 25 μM drug as follows. Cells were harvested by centrifugation, washed with phosphate buffered saline (PBS), and the centrifuged cells were resuspended in nine cell volumes of PBS. Cells were disrupted using glass beads in a Beadbeater, the extract was clarified by centrifugation at 16,000g, and absorbance was measured at 395 nm (a wavelength near the peak of NMM absorbance, but where yeast extracts absorb minimally). The absorbance of yeast extracts from untreated cells was subtracted from that from NMM-treated cells, and compared with an NMM standard to yield an approximate intracellular concentration of 5 μM. We note that this concentration is above the 1 μM Ki of NMM for inhibition of G4 DNA unwinding of Sgs1 in vitro[14], and is thus compatible with biological effects.

Supplementary Figure 4

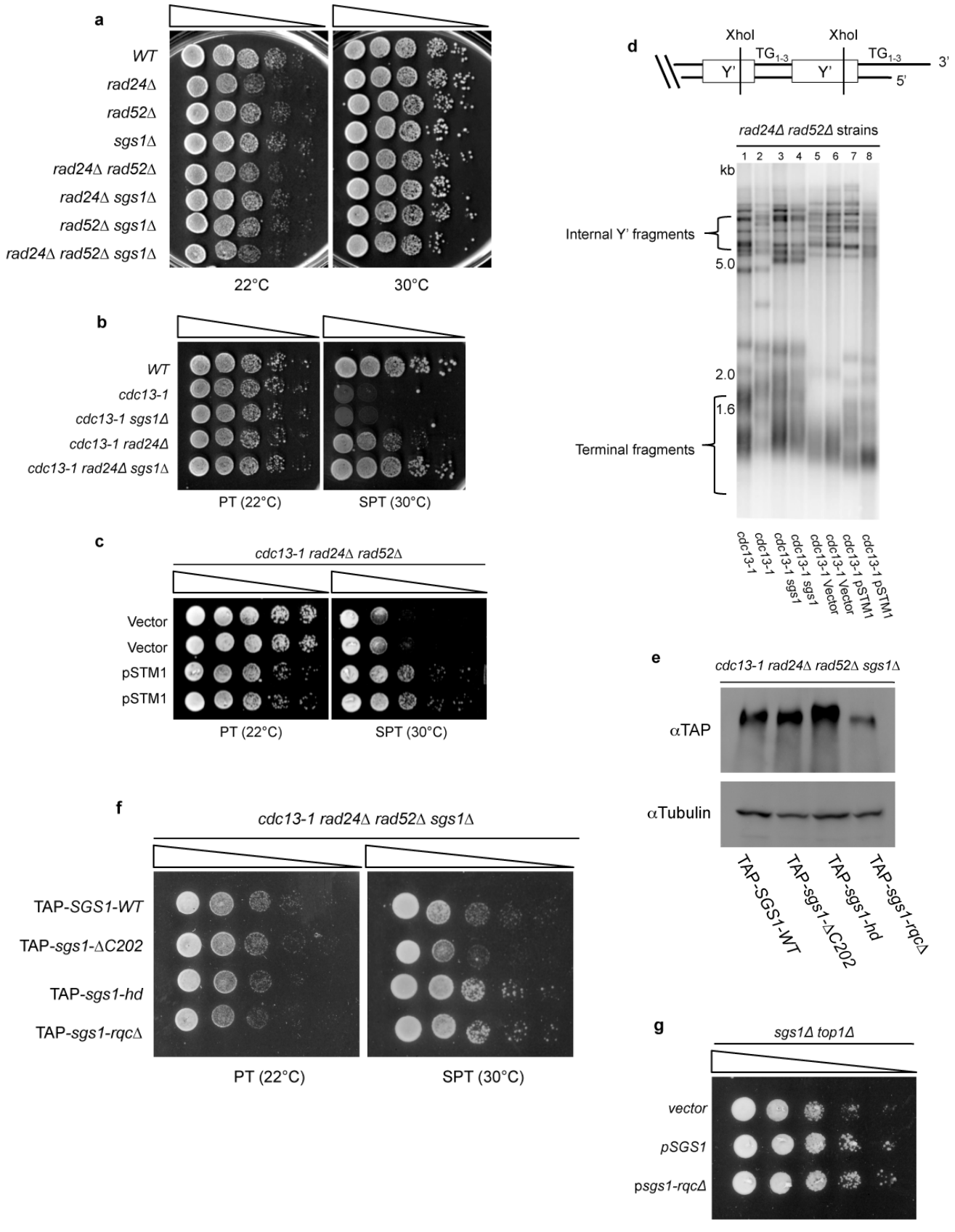

Supplementary Figure 4. Relationships of Rad24 and of Sgs1 subdomains to the rescue of the *cdc13-1* ts phenotype conferred by *sgs1* deletion. (a) In a *CDC13* background, *rad24, rad52* and *sgs1* deletions, or combinations thereof, grow similarly. **(b)** Rescue of *cdc13-1* by *sgs1* deletion does not occur in the presence of intact *RAD24.* **(c)** Rescue of the *cdc13-1* phenotype by Stm1 overexpression in a *rad24*Δ *rad52*Δ deleted background. For (a-c), 10^5 and ten-fold serial dilution of cells were spotted on YPAD (a,b) or SC-LEU (c) media and grown for 3 days at the indicated temperatures. **(d)** Telomere Southern blot of *rad24*Δ *rad52*Δ strains grown two days in liquid culture at SPT and harvested in mid-log phase. XhoI-digested DNA was denatured, blotted, and probed for yeast telomere repeats. **(e)** Anti-TAP western blot of TAP-tagged Sgs1 fusions expressed from the endogenous *SGS1* promoter in a *cdc13-1 rad24*Δ *rad52*Δ *sgs1*Δ background. Tubulin is shown as a loading control. **(f)** Spot assay of TAP-*SGS1* constructs yields the same phenotypes as untagged constructs (see **Figs. 3c-d**). **(g)** The *psgs1-rqc*Δ mutant restores normal growth to an *sgs1*Δ *top1*Δ mutant background, similar to addition of wild type *pSGS1,* indicating presence of a functional protein product. Other mutant *sgs1* alleles utilized in this study have been shown previously to possess function in similar assays[15]. 10^5 and ten-fold serial dilutions of cells were spotted on SC-HIS (f) or SC-URA (g) and grown for 3 days at 30°C.

Supplementary Figure 5

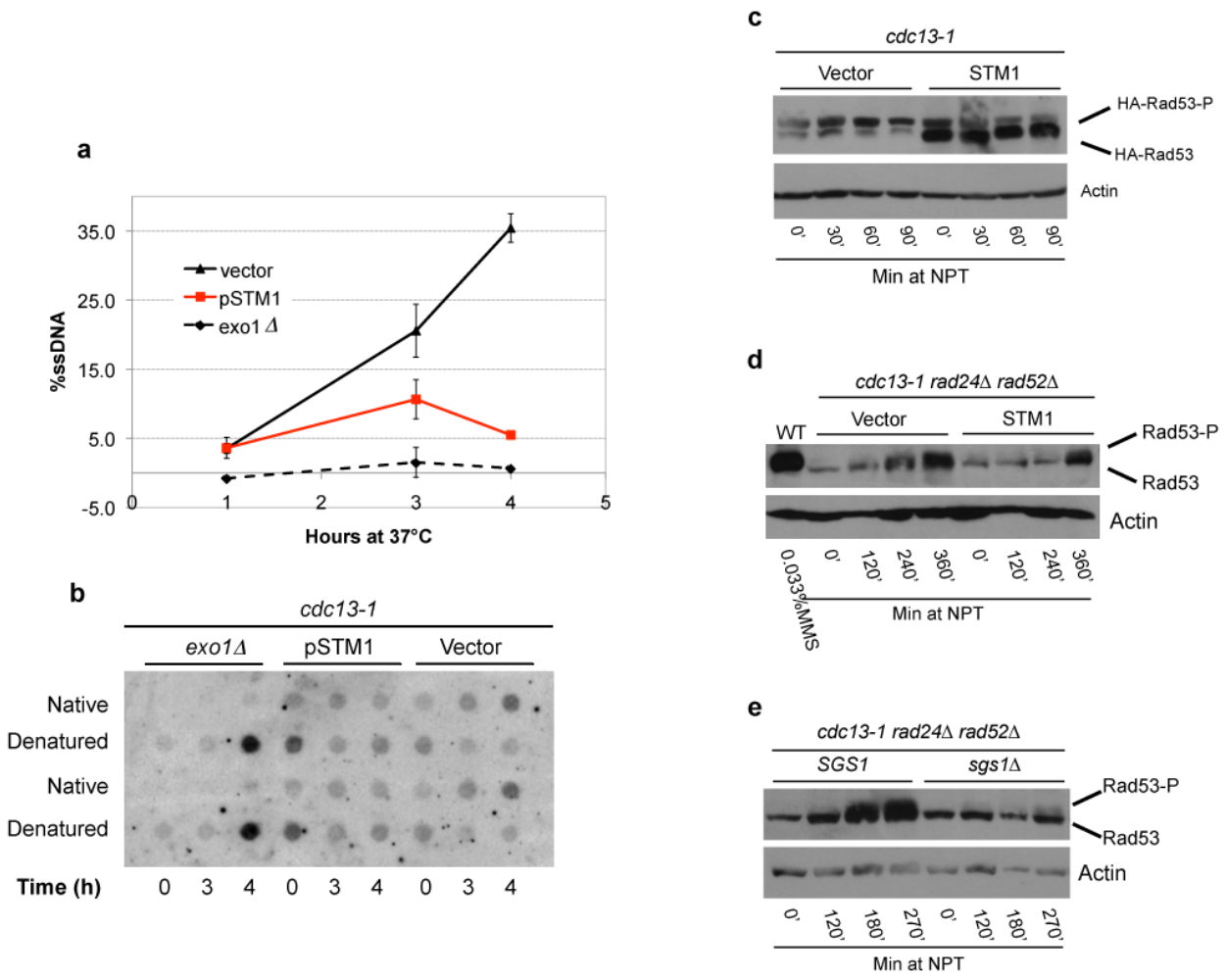

Supplementary Figure 5. Effects of *STM1* overexpression and *sgs1* deletion on telomere single strand DNA or phospho-Rad53 accumulation in *cdc13-1* mutants at NPT. (a) pSTM1 rescues resection in *cdc13-1* cells. Quantification of raw data, shown in (b). Error bars represent +/- 1SE. **(b)** Dot blot analysis of Y' subtelomeric ssDNA normalized to denatured loading controls (10% of native DNA loaded). **(c)** Rad53-dependent checkpoint activation in *cdc13-1* cells incubated for the indicated amounts of time at NPT (37°C). Endogenous *RAD53* was HA-tagged and immunoblotting was performed using an anti-HA antibody. Actin is shown as a loading control. **(d-e)** Attenuation of Rad53 phosphorylation by Stm1 overexpression (d) or *sgs1* deletion (e) in the *cdc13-1 rad24*Δ *rad52*Δ background up to four hours (d) or 4.5 hours (e) at NPT (37°C). Mid-log phase cells were grown at PT, shifted to NPT for the indicated amounts of time, and then harvested. Treatment of wild type cells with 0.033% MMS provides a positive control for Rad53 phosphorylation (d, lane 1). Note that these assays were performed at NPT (37°C) rather than SPT (30°C), which permitted faster and more extensive accumulation of shifted Rad53, and, thus, the shifted Rad53 at the latest timepoint (360') in cells with overexpressed Stm1 is consistent with the capacity of these cells to grow at SPT.

Supplementary Figure 6

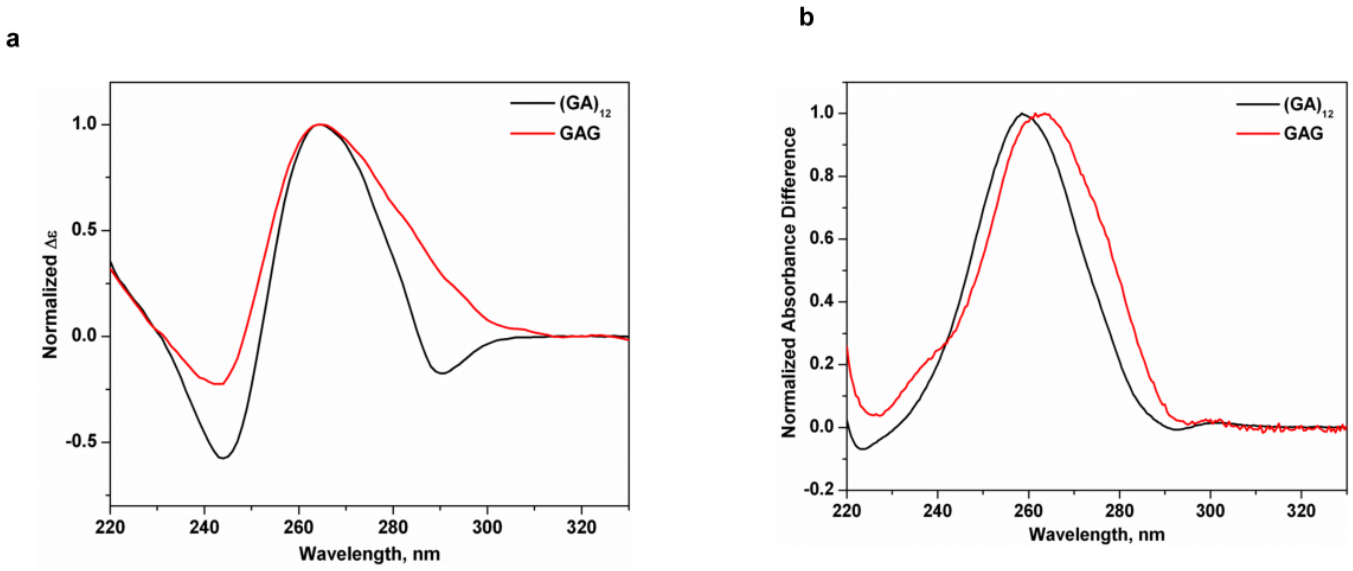

Supplementary Figure 6. The GAG oligo has CD and TDS signatures resembling those of a GA homoduplex. **(a)** Normalized CD spectra of a homoduplex-forming $(GA)_{12}$ oligo and the $(TGTGAG)_4$ overhang oligo. **(b)** Normalized thermal difference spectra (TDS) of the $(GA)_{12}$ oligo and the $(TGTGAG)_4$ oligo.

Supplementary Figure 7

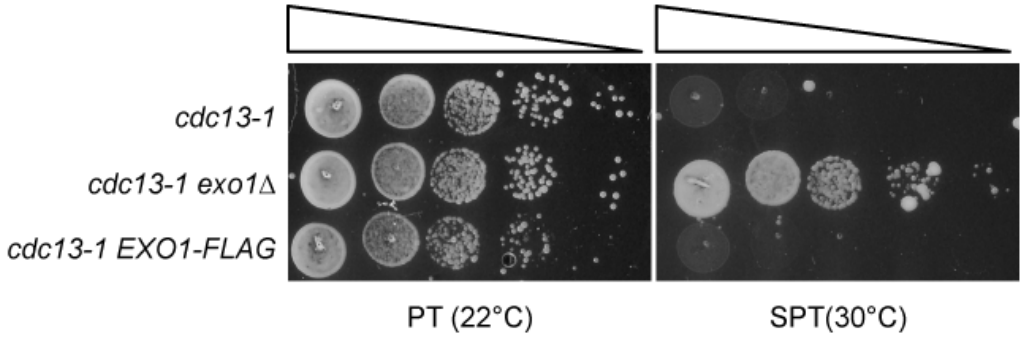

Supplementary Figure 7. Exo1-FLAG functions like endogenous Exo1 in a *cdc13-1* growth assay. Replacement of endogenous Exo1 with Exo1-FLAG yields a growth defect in *cdc13-1* cells comparable to *cdc13-1* strains possessing untagged Exo1, and in contrast to the rescue of growth afforded by *exo1* deletion in *cdc13-1* cells. 10^5 and ten-fold serial dilutions of samples were spotted on YPAD and grown 3 days at the indicated temperatures.

Nature Structural & Molecular Biology: doi:10.1038/nsmb.2033

Supplementary Figure 8

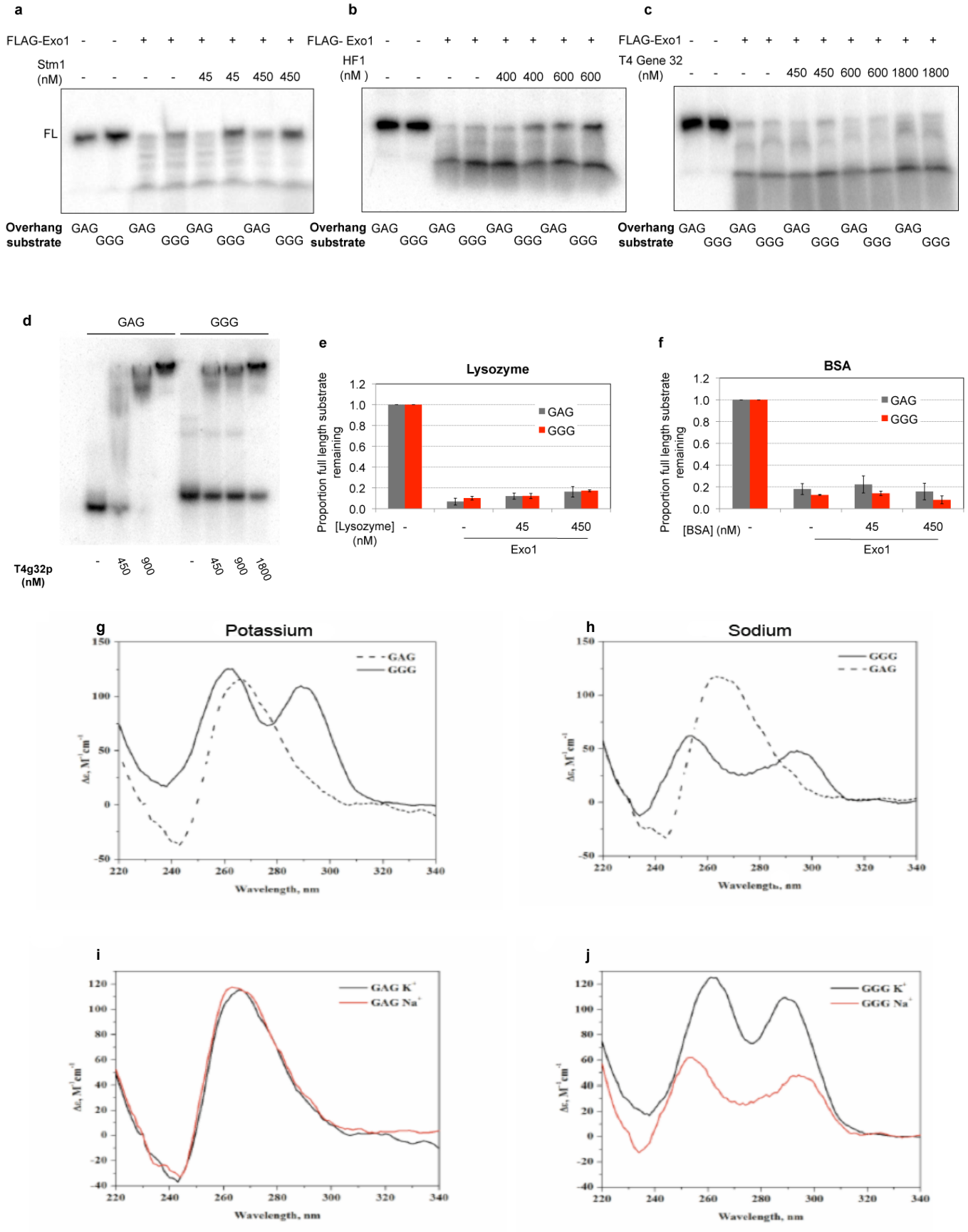

Supplementary Figure 8. G4 DNA binding proteins selectively protect against exonuclease degradation of a model telomere substrate. Denaturing polyacrylamide gel electrophoresis-based assessment of protection of synthetic telomere substrates by **(a)** Stm1 **(b)** the scFv antibody HF1 or **(c)** T4 gene 32 protein. For each assay, 220 fmol of duplex substrate was pre-incubated at 30°C with the indicated concentrations of Stm1 (a), HF1 (b) or T4 gene 32 protein (c), and then treated with 3 pmol Exo1-FLAG for 20 min at room temperature. *FL* = full-length bottom strand. We confirmed normal function of Exo1-FLAG by knocking it into the endogenous *EXO1* locus in a *cdc13-1* background, and demonstrating that *cdc13-1 EXO1-FLAG* strains have the same ts growth as *cdc13-1 EXO1* strains (Supplementary Fig. 7). **(d)**T4 gene 32 protein (T4g32p) binds to both the GAG and GGG overhang at concentrations used in the exonuclease assay (see Fig. 6f). An electromobility shift assay (EMSA) was performed using the same concentrations of protein and oligo and the same buffer conditions as that in the exonuclease assay. Reactions were run on a 12% polyacrylamide gel under non-denaturing conditions. Note that not all of the GGG oligo was shifted, which may reflect an inability of T4g32p to bind the G-quadruplex conformation of the oligo. **(e, f)** Control proteins, lysozyme and BSA, do not inhibit Exo1 activity on G4 DNA (GGG) or control (GAG) overhang templates *in vitro.* Exonuclease assays were performed as in Fig. 6, but in the presence of increasing amounts of lysozyme (e) or BSA (f). Data from two independent experiments for each protein are shown with standard errors. **(g)** CD spectra of the GGG and GAG oligos incubated at 30°C in 100 mM K^+ Exo1 buffer (see *Methods*). The GGG oligo formed a mixture of parallel and antiparallel G4 DNA while the GAG oligo had a spectrum similar to a GA homoduplex. **(h)** CD spectra of the GGG and GAG oligos incubated at 30°C in 100 mM Na^+ Exo1 buffer. GGG formed a mixture of G4 DNA structures, but with lower peak signals than in the K^+ buffer. GAG yielded a spectrum similar to a GA homoduplex. **(i, j)** Comparisons of CD spectra of the GAG or GGG oligos, respectively, in K^+ *vs*. Na^+ Exo1 buffer. Data are the same as those shown in (g) and (h), but have been recombined to facilitate comparisons. Note that the GAG spectrum is independent of the type of monovalent cation, in contrast to the GGG oligo which has a G-quadruplex spectrum stabilized by K^+, further supporting our conclusion that the GAG sequence does not form a G-quadruplex.

Supplementary Table I. List of strains used in this study.

Strain	Genotype	Reference
YBJ1	PSY316 (*ade2-101 his3Δ200 leu2-3, 2-112 lys2 ura3-52)* MATα	Park et al., 1999
YBJ120	YBJ1 *cdc13-1*	This study
YBJ3	YBJ1 *sgs1∆::hisG'*	This study
YBJ122	YBJ120 *sgs1∆::hisG'*	This study
QCY112	YBJ120 YEplac181-*STM1*	This study
QCY116	YBJ120 YEplac181	This study
QCY175	PSY316 *MAT a/α CDC13/cdc13-1 RAD52/rad52Δ::HygB RAD24/rad24∆::kanMX SGS1/sgs1Δ::hisG'*	This study
QCY169	YBJ120 *rad52::HygB rad24::kanMX* YEplac181	This study
QCY171	YBJ120 *rad52::HygB rad24::kanMX* YEp*STM1-LEU2*	This study
QCY197	YBJ120 *rad52::HygB rad24::kanMX*	This study
QCY196	YBJ120 *rad52::HygB rad24::kanMX sgs1Δ::hisG'*	This study
QCY198	YBJ1 *rad52::HygB rad24::kanMX*	This study
JSY1004	15Daub *stn1Δ::TRP1* YEp111-*stn1-154*	Grandin et al., 2001
JSY1014	JSY1004 YEplac195-*STM1*	This study
JSY1016	JSY1004 YEplac195	This study
JSY28	QCY196 pRS416	This study
JSY27	QCY196 pRS416-*SGS1*	This study
JSY26	QCY 196 p*sgs1-ΔC200-URA3*	This study
JSY48	QCY196 p*sgs1-ΔC300-URA3*	This study
JSY49	QCY196 p*sgs1-ΔC400-URA3*	This study
JSY50	QCY196 p*sgs1-ΔC500-URA3*	This study
JSY51	QCY196 p*sgs1-ΔC795*	This study
JSY33	QCY196 pRS415	This study
JSY54	QCY196 p*SGS1-LEU2*	This study
JSY55	QCY196 p*sgs1-ΔC202-LEU2*	This study
JSY56	QCY196 p*sgs1-hd-LEU2*	This study
JSY59	QCY196 p*sgs1-Δrqc-URA3*	This study
JSY57	QCY196 p*RAD52-URA3*	This study
JSY58	QCY197 p*RAD52-URA3*	This study
JSY114	JSY58 *rmi1Δ::HIS3*	This study
JSY116	JSY57 *rmi1Δ::HIS3*	This study
JSY118	JSY58 *top3Δ::HIS3*	This study
JSY120	JSY57 *top3Δ::HIS3*	This study
JSY122	JSY57 *tlc1Δ::NAT* p*TLC1-HIS3*	This study
JSY128	JSY57 *tlc1Δ::NAT* p*tlc1-uCu-HIS3*	This study
JSY125	JSY57 *tlc1Δ::NAT* p*tlc1-CuA-HIS3*	This study
JSY154	JSY58 *tlc1Δ::NAT* p*TLC1-HIS3*	This study
JSY158	JSY58 *tlc1Δ::NAT* p*tlc1-uCu-HIS3*	This study
JSY160	JSY58 *tlc1Δ::NAT* p*tlc1-CuA-HIS3*	This study
JSY0115	BY4742: MATα *his3Δ1 leu2Δ0 ura3Δ0 met15Δ0*	Brachmann et al., 1998.

JSY0116	JSY0115 *cdc13-1*	This study
JSY0126	JSY0116 YEp*STM1-LEU2*	This study
JSY0128	JSY0116 YEplac181	This study
JSY1000	JKM111 derivative: *MAT a/α hoΔ/hoΔ hmlΔ::ADE1/hmlΔ::ADE1 hmrΔ::ADE1/ΔhmrΔADE1 ade1/ade1 leu2-3,112/leu2-3,112 lys5/lys5 ura3-52/ura3-52*	Moore and Haber, 1996
JSY1033	JSY1000 *sgs1Δ::hisG' top1Δ::HygB* pRS416	This study
JSY1034	JSY1000 *sgs1Δ::hisG' top1Δ::HygB* pRS416-*SGS1*	This study
JSY1040	JSY1000 *sgs1Δ::hisG' top1Δ::HygB* pRS416-*sgs1-Δrqc*	This study
JSY241	YBJ122 pAG413-*GAL*-5xHA	This study
JSY242	YBJ122 pAG413- *GAL*-5xHA-*sgs1-RQC*	This study
JSY265	YBJ3 pAG413- *GA1*-5xHA	This study
JSY263	YBJ3 pAG413- *GAL*-5xHA- *sgs1-RQC*	This study
JSY258	YBJ1 *rad52Δ::HygB*	This study
JSY274	QCY112 *rad52Δ::HygB*	This study
JSY276	QCY116 *rad52Δ::HygB*	This study
JSY289	JSY24 *rad52Δ::HygB*	This study
JSY291	JSY25 *rad52Δ::HygB*	This study
JSY296	YBJ1 pAG413- *GAL*-5xHA-*HF1*	This study
JSY298	YBJ120 pAG413- *GAL*-5xHA-*HF1*	This study
JSY300	QCY198 pAG413- *GAL*-5xHA-*HF1*	This study
JSY302	QCY197 pAG413- *GAL*-5xHA-*HF1*	This study
JSY233	QCY198 pAG413- *GAL*-5xHA	This study
JSY237	QCY197 pAG413- *GAL*-5xHA	This study
JSY326	YBJ1 pAG416-*GAL*-13xMyc	This study
JSY335	YBJ1 pAG416-*GAL*-13xMyc-*HF1*	This study
JSY329	YBJ120 pAG416-*GAL*-13xMyc	This study
JSY339	YBJ120 pAG416-*GAL*-13xMyc-*HF1*	This study
JSY386	QCY175 spore product: *CDC13 rad24Δ::kanMX RAD52 SGS1*	This study
JSY388	QCY175 spore product: *CDC13 RAD24 RAD52 sgs1Δ::hisG'*	This study
JSY390	QCY175 spore product: *CDC13 rad24Δ::kanMX RAD52 sgs1Δ::hisG'*	This study
JSY391	QCY175 spore product: *CDC13 rad24Δ::kanMX rad52Δ::HygB sgs1Δ::hisG'*	This study
JSY392	QCY175 spore product: *CDC13 RAD24 rad52Δ::HygB sgs1Δ::hisG'*	This study
JSY377	QCY196 pAG413-TAP-*SGS1-HIS3*	This study
JSY379	QCY196 pAG413-TAP-*sgs1-ΔC202-HIS3*	This study
JSY381	QCY196 pAG413-TAP-*sgs1-hd-HIS3*	This study
JSY383	QCY196 pAG413-TAP-*sgs1-Δrqc-HIS3*	This study

Methods

Yeast Strains and Plasmids

Unless indicated otherwise, strains were derived from the PSY316 background[1]; see **Supplementary Table 1** for complete list of strains. Cells were cultured in YPAD or synthetic complete (SC) media as described[2]; temperature sensitive strains were propagated at room temperature (22°C) whereas other strains were grown at 30°C. Gene deletions and knock-in mutations were performed using standard genetic methods[2]. In *rad52Δ* strains, HR-based genome alterations were achieved by transformation with a counter-selectable p*RAD52-URA3* plasmid prior to transformation with knock-out or knock-in DNA, followed by selection for *RAD52* plasmid loss on 5-fluoroorotic acid (5-FOA). For strains in which telomerase RNA (*TLC1*) was deleted and replaced by plasmid-based alleles, *TLC1* was deleted in *cdc13-1 rad24Δ rad52Δ pRAD52-URA3* cells, primary colonies were immediately selected on 5-FOA, and resistant cells transformed with p*TLC1* plasmids so that cells lacked telomerase for ~45-50 cell divisions. p*TLC1* template mutant, p*SGS1* mutant, and the YEpT*STM1* plasmids were kindly provided by Liz Blackburn, Stephen Brill, and Seishi Murakami respectively. YEplac181-*STM1* and YEplac195-STM1 were generated by cloning the 4.85 kb SacI – EcoRI fragment from YEpT*STM1* into the same sites of YEplac181 or YEplac195, respectively. The p*SGS1* constructs were cloned from a pRS405 backbone into the ARS/CEN vectors pRS416 and pRS415. The p*sgs1-rqcΔ* plasmid was generated from WT p*SGS1* using a two-round PCR-based strategy that precisely deleted amino acids 1005-1212. The Sgs1 *RQC* and *HF1* overexpression constructs were generated by PCR amplification of the desired coding region with primers possessing an N-terminal SV40 NLS, followed by Gateway (Invitrogen) recombination-based cloning into a *GAL1*-driven ARS-CEN vector (pAG413-GAL or pAG416) possessing an N-terminal 5xHA tag or 13XMyc tag.

Single-stranded DNA Quantification

Log phase cells growing at 22°C were arrested at G2/M by treatment with 20 µg/ml nocodazole for 3h, diluted 1:3 with media pre-warmed to 55°C, and shifted to NPT (37°C) with continued nocodazole arrest. Cells were harvested at the indicated time points, and DNA was isolated by a standard purification method using glass bead lysis and phenol-chloroform extraction[3]. Detection and quantification of single-stranded DNA was performed as described in Garvik et al., 1995[4] with the following alterations. Undigested native DNA (2 µg) or DNA denatured in 0.2 M NaOH at 65°C (0.2 µg), was diluted to a final volume of 300 µl with 10x SCP buffer (1 M NaCl, 0.3 M Na_2HPO_4, 0.02 M EDTA pH 6.8) and incubated for 15 min on a Hybond-XL membrane using a dot-blotting apparatus. Samples were then drawn through the membrane by application of a vacuum, followed by 3 washes with TMAC wash buffer (3.0 M TMAC, 50 mM Tris-HCl, 0.1 mM EDTA, pH 8.0); TMAC was used to destabilize secondary structures that might inhibit probe binding. DNA was then crosslinked to the membrane using a 254 nm Stratalinker (12 µJ x 100), and the membrane was prehybridized at 55°C in buffer containing 6X SSC, 5X Denhart's Buffer, 20mM sodium phosphate (pH 7.0), and 25µg/ml boiled salmon sperm DNA. Blots were washed 4 x 5 min with TMAC hybridization buffer (3M TMAC, 5X Denhart's Buffer, 50 mM Tris-HCl pH 8.0, 10 µg/ml salmon sperm DNA, 0.1 mM EDTA pH 8.0 0.6% lithium dodecyl sulfate). An oligonucleotide probe specific for Y' subtelomeric DNA continuous with the G-rich telomere strand (5'-TCGTGTTATCTGCAGCGAGAACTTCAACGTTTGCC-3') was end-labeled with γ -^{32}P-ATP using T4 polynucleotide kinase, and hybridized overnight to the membrane in TMAC hybridization buffer at 65°C. Membranes were washed 3 times for 5 min at room temperature (22°C) in TMAC wash buffer, and imaged and quantified with a Molecular Dynamics Phosphorimager and ImageQuant analysis software.

G-quadruplex Ligand Assays

Drugs used in this study include bisquinolinium compounds Bipy-DC6 and Phen-DC6[5], ethidium bromide, mesoporphyrin IX and *N*-methyl mesoporphyrin IX (MP and NMM; Frontier Scientific). To perform assays, log growth cultures in synthetic complete (SC) media were diluted to 4 x 10^5 cells/ml in 1.5 ml of culture containing the indicated concentrations of drug or DMSO vehicle control. Cultures were grown for 24h (NMM, and MP) or 30h (Bipy-DC6 and Phen-DC6) at 30°C, and cell density was quantified using a Beckman Coulter Counter.

In vitro Exonuclease Assays

Partial duplex telomeric substrates were formed using 35 pmol each of HPLC-purified top (GGG: 5'-BIO/GTACTTATTTCGGAATGAGCTTCATAAGATAATGGTCAGATCAATA TGAGA$(TGTGGG)_4$-3';
GAG: 5'-BIO/GTACTTATTTCGGAATGAGCTTCATAAGATAATGGTCAGATCAAT ATGAGA$(TGTGAG)_4$-3') and bottom oligo (5'-TCTCATATTGATCTGACCATTATCTTA TGAAGCTCAT TCCGAAATAAGTA–3') diluted in 15 µl TEM buffer (10 mM Tris 8.0, 1mM EDTA, 10 mM $MgCl_2$) denatured at 94°C for 5 min, and annealed by shifting to 79°C and decreasing temperature at 1°C/min to 55°C, followed by 55°C for 3 hr. Duplex substrates were then end-labeled by mixing 7.5 µl duplex, 2 µl 10X buffer (100 mM Tris-Cl, 500 mM NaCl, 100 mM $MgCl_2$, 10 mM DTT, pH 7.9), 9 µl H_2O, 1 µl (5 u) Klenow (3'-> 5' exo^-) and 0.5 µl α-^{32}P-dCTP and incubating for 30 min at 30°C. Unincorporated dCTP was removed by gel filtration with columns pre-swollen in TE 8.0 with 100 mM KCl, and samples were diluted with approximately 60 µl H_2O to a final volume of 80 µl. To promote G-quadruplex formation, 220 fmol (1 µl) of duplex substrate was incubated for 20 min at 30°C in a final volume of 15 µl of Exo1 buffer (100 mM KCl, 25mM Tris-HCl pH 8.0, 10 mM $MgCl_2$, 1 mM DTT, 4% glycerol, and 100 µg/ml BSA) and containing the indicated amounts of Stm1, T4 gene 32 protein (NEB), lysozyme, or BSA. Exonuclease digestion was performed by addition of 3 pmol of Exo1 in 10 µl of Exo1 buffer and incubation at room temperature for 20 min. Reactions were stopped by addition of 5 µl 80% formamide/0.1% bromophenol blue/0.1% xylene cyanol), boiled for 8 min, and separated on 8 M urea, 8% acrylamide gels run in 0.5X TBE. Phosphorimager images of gels were quantified using ImageJ analysis software.

Electromobility Shift Assays (EMSAs)

EMSAs for T4 gene 32 protein were performed by incubating the indicated amounts of protein with 220 fmol of 5'-^{32}P end labeled GAG or GGG overhang oligo ($(TGTGAG)_4$ or $(TGTGGG)_4$ resepectively). Binding reactions were performed in ExoI buffer (see In vitro exonuclease assays) for 20 min at 30°C. Samples were separated on a 12% non-denaturing acrylamide gel run at 130V in 0.5X TBE at 4°C.

Spot Assays

Spot assays were performed using cultures growing in log phase. Beginning with 10^5 cells/spot, ten-fold serial dilutions were spotted onto YPAD, or, for strains possessing plasmids, the relevant selective SC media, and grown at 22°C (PT) or at 28°C - 30°C as indicated (SPT) for the indicated number of days. We note that rescue of *cdc13-1* mutant growth at SPT by YEp*STM1* was observed in YPD and SC media prepared according to Amberg et al. [2], but not in a more minimal SC medium lacking alanine, aspartate, cysteine, glutamine, glutamate, glycine, inositol, PABA, proline, serine, and threonine (M. Chang and R. Rothstein, *personal communication*).

Telomere Southern Blot

Telomere Southern analysis was performed as described previously[6]. Briefly, XhoI-digested genomic DNA was separated on a 1% agarose gel, denatured under alkaline

conditions, and transferred to Hybond-XL membrane. A radiolabeled probe against the *S. cerevisiae* TG_{1-3} telomere repeat was used to detect total telomeric DNA. Blots were imaged with a Molecular Dynamics Phosphorimager.

Immunoblots

Log phase cultures grown at room temperature were diluted 1:3 with medium prewarmed at 55°C at the start of the 37°C time course. Samples were harvested at the specified time intervals and protein was isolated using mechanical disruption of cells in the presence of 20% TCA [7]. Lysates were run on 4-12% SDS-PAGE gradient gels and transferred to PVDF membrane. Blots were probed with 1:1000 anti-Rad53 (generously provided by Dan Durocher), 1:150 anti-Rad53 (yC-19; Santa Cruz sc-6749), 1:200 anti-HA tag (Y-11; Santa Cruz sc805), 1:1000 anti-alpha tubulin (YL 1/2; Abcam ab6160) or 1:1000 Actin (I-19; Santa Cruz sc-1616) followed by 1:5000 anti-goat-HRP secondary (Santa Cruz sc2020), 1:2500 anti-rat-HRP (Jackson Immunoresearch, 112-035-167) or 1:1000 ECL-rabbit secondary (GE Healthcare, NA9340) antibody. All incubations and washes were performed in 150 mM NaCl, 50 mM Tris pH 7.6 containing 5% BSA and 0.2% Tween 20 or 1% milk and 0.1% Tween 20.

Chromatin Immunoprecipitation

Chromatin immunoprecipitation was performed as described[8]. Briefly, cells growing at mid-log phase were crosslinked with 1% formaldehyde. Reactions were stopped with 125 mM glycine at RT for 5 min, and cells were washed with 1x PBS. Pellets were then resuspended in FA-Lysis buffer (50 mM Hepes-KOH 7.5, 140 mM NaCl, 1 mM EDTA, 0.1% TritonX-100, 1 mM PMSF, 2 µg/ml aprotinin, 2 µg/ml leupeptin, 2 µg/ml pepstatin A) and ~500 µl zirconia/silica beads and homogenized with a mini-beadbeater (BioSpec) (3 x 90 sec). Lysate was sonicated with a Bioruptor (30 sec on/30 sec off for 20 min), and immunoprecipitations were performed on 0.4 mg protein with an HA tag antibody (abcam cat# ab9110) or a Myc tag antibody (Abcam cat# ab9132). Six washes were performed (2 x FA-Lysis buffer, 1 x FA-Lysis buffer/500 mM NaC, 2 x LiCl solution (10 mM Tric-HCl, pH 8.0, 0.25M LiCl, 1mM EDTA, 0.5% NP-40), 1 x TE 8.0), followed by reverse crosslinking at 65°C in the presence of 0.2M NaCl. Following RNaseA, and proteinase K treatment, DNA was purified using a Qiagen PCR purification kit, and qPCR was performed using the Syber Green Jumpstart Taq ReadyMix (Sigma) on a Roche LightCycler 480.

Telomere Sequencing

Telomere sequencing was performed as described previously[9]. Briefly, total yeast genomic DNA was purified using glass bead lysis and two phenol/chloroform/isomamyl alcohol extractions followed by a final chloroform extraction. Telomeres were C-tailed using terminal deoxynucleotidyl transferase (45 min at 37°C, 10 min at 65°C, 5 min at 96°C) and the Chr. IL telomere was PCR amplified using 1 forward and 2 reverse primers (O286s MluI: 5'-CACGCGTGGTTGGCCAGGGTTAGATTAGGGCTG-3', G18A-BamHI: 5'-CGGGATCCGGGGGGGGGGGGGGGGGGA-3', G18C-BamHI 5'-CGGG ATCCGGGGGGGGGGGGGGGGGGC-3') with AccuPrime GC-Rich DNA Polymerase (Invitrogen, Cat# 12337016), cloned into pSC-A-amp/kan vectors using a StrataClone PCR cloning kit (Cat# 240205), and sequenced.

Circular Dichroism

Circular dichroism spectra (Figs. 5 and 6) were collected using an AVIV 410DS spectrometer equipped with a Peltier heating unit with the following settings: path length, 0.2 -1 cm; windows, 220 nm – 350 nm, temperature, 25°C; averaging time, 1 second; and total of 5 scans. To determine molar ellipticity, UV/Vis data were collected using a Cary300 Varian UV-

Vis Spectrophotometer. Data were analyzed using Origin analysis software. For Fig. 5, oligonucleotides were prepared by heating 25 mM oligonucleotide in 10 mM K_2HP0_4 pH 7, 100 mM KCl to 100^0C for three minutes, transferring to 75^0C and slowly cooling to 30^0C overnight, followed by dilution in the same buffer to 5mM for CD studies. Thermal denaturation of DNA was followed by monitoring the CD absorbance at 263 nm (for oligonucleotides 1, 1-corr, 2, and 2-corr) or 290 nm (for oligonucleotides 3, 3-corr, 4, and 4-corr) in a 1-cm cell. The accuracy of the external temperature probe was ±0.3 K, the heating rate was set at 10ºC min^{-1}, equilibration time was 1 min (resulting in the overall temperature increase rate of 0.33ºC min^{-1}), temperature range was 5 – 95ºC and down to 5ºC, response averaging time was 10 s, and bandwidth was 1 nm. The data analysis[10] yielded the transition temperature T_m, the enthalpy of unfolding ΔH, and the free energy of unfolding at room temperature ΔG_u(25ºC). Fits were performed assuming a two-state equilibrium between native and unfolded state, N ↔ U, and constant ΔH ($\Delta C_P = 0$). Fits did not improve upon including a non-zero ΔC_P. For Fig. 6, oligonucelotides (5 mM) were prepared in the same fashion as the DNA used in the exonuclease assays (annealing TEM buffer, followed by 30°C incubation for 30 minutes after 100 mM KCl addition; see above). For Supplemental Fig. 2, circular dichroism spectra were obtained on a Chirascan spectrophotometer from Applied Photophysics using 1 mm pathlength cuvets. The wavelength was varied from 220 to 320 nm. Measurements were made at 25°C. Each spectrum reported is an average of 4 scans. The samples were prepared to a final oligonucleotide and HF1 concentration of 1 μM in 50 mM Tris-HCl (pH 7.4) and 100 mM KCl. For each experiment, a CD spectrum of the buffer was recorded and subtracted from the spectrum obtained from the DNA-containing solution.

UV-Vis Analysis of Thermal Difference Spectra

UV-Visible spectroscopy data were collected on a Cary 300 Varian Spectrophotometer. Thermal Difference Spectra (TDS) were obtained by subtracting the low temperature (where DNA structure is stable) spectrum from the high temperature spectrum (where DNA is denatured). The spectra are displayed as the difference between molar extinction coefficients for the ease of comparison of various DNA structures. In some cases the TDS spectra were normalized assigning a value of +1 to the highest positive peak. Data analysis was performed using Origin software.

FRET Analysis

Fluorescently labeled DNA sequence, FGD, 5′– FAM-GGG(TGTGGG)$_3$-Dab–3′ and FAD, 5′–FAM-GAG(TGTGAG)$_3$-Dab–3′, were purchased from Integrated DNA Technologies (IA, USA). 6-FAM is 6-carboxyfluorescein and Dabcyl is 4,4-dimethylamino-azobenzene-4'-carboxylic acid. DNA was diluted with MilliQ water to a final concentration of 0.1-0.2 mM and stored at -80ºC. The concentration of oligonucleotides was determined using the sum of extinction coefficients for the DNA, Dabcyl and 6-FAM(FGD, ε_{260} = 233,343 $M^{-1}cm^{-1}$ and for FAD ε_{260} = 250,100 $M^{-1}cm^{-1}$). The oligonucleotides were annealed according to the procedure used to prepare oligonucleotide for Exo1 assay (concentration was kept at 25 μM during both annealing steps). Samples were diluted to a final concentration of 0.2 μM in TEM buffer with 100 mM KCl. FRET measurements were carried out on a Spex Fluorolog-3 (HORIBA Jobin Yvon, France) at 25°C in 1×1 cm quartz cuvette using 2050 μL sample volume. Fluorescence spectra were collected using an extication wavelength of 470 (slit width 5 nm) and an emission wavelength of 500-600 nm (slit width 10 nm), with 1 scan, 1nm step size, and 1 sec averaging time. Lamp fluctuations were corrected by using the reference channel. Stm1 or BSA were diluted with TEM buffer, 100 mM KCl to 25 μM right before expreiment. The appropriate amount of protein was added to DNA solution, mixed thoroughly and incubated for 1h at 25°C. Thorough mixing

was also required to correct for possible photobleaching. Collected spectra were corrected for DNA dilutions.

Protein Expression and Purification

Stm1 was expressed and purified as described previously[11]. Briefly, a 6xHis N-terminally tagged pETSTM1, generously provided by Michael W. Van Dyke, was expressed in IPTG inducible BL21 cells. Recombinant protein was purified with nickel affinity chromatography. A slightly modified version of pFB-EXO1-FLAG, described previously[12], was constructed by PCR amplifying *EXO1* from yeast genomic DNA using the primers 5'-AGCCTCGAGCCATGGGTATCCAAGGTCTTCTTCCTC-3' and 5'-AGCAAGCTTCTCGAGTTACTTATCGTCGTCATCCTTGTAATCTTTACCTTTATAAACAAAT TGGGAAAG-3', which inserted the FLAG sequence directly before the *EXO1* stop codon. The PCR product was digested with XhoI and HindIII and inserting into pFastBac1, prepared with the same enzymes. The C-terminally FLAG-tagged protein was expressed in *Spodoptera frugiperda (Sf9)* cells infected with recombinant Exo1-FLAG baculovirus and purified using anti-FLAG affinity chromatography as described [12].

Supplemental References

1. Park, P.U., Defossez, P.A. & Guarente, L. Effects of mutations in DNA repair genes on formation of ribosomal DNA circles and life span in *Saccharomyces cerevisiae. Mol. Cell. Biol.* **19**, 3848-3856 (1999).
2. Amberg, D.C., Burke, D.J. & Strathern, J.N. *Methods in Yeast Genetics 2005*, (Cold Spring Harbor Laboratory Press, Cold Spring Harbor, NY, 2005).
3. Hoffman, C. & Winston, F. A ten-minute DNA preparation from yeast efficiently releases autonomous plasmids for transformation of Escherichia coli. *Gene* **57**, 267-72 (1987).
4. Garvik, B., Carson, M. & Hartwell, L. Single-stranded DNA arising at telomeres in cdc13 mutants may constitute a specific signal for the RAD9 checkpoint. *Mol. Cell. Biol.* **15**, 6128-6138 (1995).
5. De Cian, A., DeLemos, E., Mergny, J.-L., Teulade-Fichou, M.-P. & Monchaud, D. Highly Efficient G-Quadruplex Recognition by Bisquinolinium Compounds. *Journal of the American Chemical Society* **129**, 1856-1857 (2007).
6. Lee, J.Y., Mogen, J.L., Chavez, A. & Johnson, F.B. Sgs1 RecQ Helicase Inhibits Survival of Saccharomyces cerevisiae Cells Lacking Telomerase and Homologous Recombination. *J. Biol. Chem.* **283**, 29847-29858 (2008).
7. Wright, A.P., Bruns, M. & Hartley, B.S. Extraction and rapid inactivation of proteins from Saccharomyces cerevisiae by trichloroacetic acid precipitation. *Yeast* **5**, 51-3 (1989).
8. Kozak, M.L. et al. Inactivation of the Sas2 histone acetyltransferase delays senescence driven by telomere dysfunction. *EMBO J* **29**, 158-170.
9. Forstemann, K., Hoss, M. & Lingner, J. Telomerase-dependent repeat divergence at the 3' ends of yeast telomeres. *Nucl. Acids Res.* **28**, 2690-2694 (2000).
10. Ramsay, G.D. & Eftink, M.R. Analysis of multidimensional spectroscopic data to monitor unfolding of proteins. *Methods Enzymol* **240**, 615-45 (1994).
11. Nelson, L.D., Musso, M. & Van Dyke, M.W. The Yeast STM1 Gene Encodes a Purine Motif Triple Helical DNA-binding Protein. *J. Biol. Chem.* **275**, 5573-5581 (2000).
12. Tran, P.T., Erdeniz, N., Dudley, S. & Liskay, R.M. Characterization of nuclease-dependent functions of Exo1p in Saccharomyces cerevisiae. *DNA Repair* **1**, 895-912 (2002).

13. Fernando, H., Rodriguez, R. & Balasubramanian, S. Selective Recognition of a DNA G-Quadruplex by an Engineered Antibody,Ä†. *Biochemistry* **47**, 9365-9371 (2008).
14. Huber, M.D., Lee, D.C. & Maizels, N. G4 DNA unwinding by BLM and Sgs1p: substrate specificity and substrate-specific inhibition. *Nucl. Acids Res.* **30**, 3954-3961 (2002).
15. Mullen, J.R., Kaliraman, V. & Brill, S.J. Bipartite Structure of the SGS1 DNA Helicase in Saccharomyces cerevisiae. *Genetics* **154**, 1101-1114 (2000).